

# Autonomous Spilled Oil and Gas Tracking Buoy System and Application to Marine Disaster Prevention System

M.FUJIHARA<sup>1</sup>, N. KATO<sup>1</sup>, H. SENGA<sup>1</sup>, H. SUZUKI<sup>1</sup>, Y. OKANO<sup>2</sup>, T. BAN<sup>2</sup>,  
Y. TAKAGI<sup>2</sup>, M. YOSHIE<sup>3</sup>, T. TANAKA<sup>3</sup>, N. SAKAGAMI<sup>4</sup>

- <sup>1</sup> Osaka University, Graduate School of Engineering  
<sup>2</sup> Osaka University, Graduate School of Engineering Science  
<sup>3</sup> Port and Airport Research Institute  
<sup>4</sup> Tokai University, Faculty of Marine Science & Technology

## Abstract

This paper describes the ongoing project on autonomous spilled oil and gas tracking buoy system and application to marine disaster prevention system for 5 years since FY2011 (<http://www.naoe.eng.osaka-u.ac.jp/~kato/project/>). The objectives of this project are as (1) autonomous tracking and monitoring of spilled plumes of oil and gas from subsea production facilities by an underwater buoy robot, (2) autonomous tracking of spilled oil on the sea surface and transmission of useful data to a land station through satellites in real time by multiple floating buoy robots, (3) improvement of the accuracy of simulations for predicting diffusion and drifting of spilled oil and gas by incorporating the real-time data from these robots. This paper describes the first and second items on developments of robots.

**Keywords:** oil, gas, underwater buoy robot, autonomous tracking, multiple floating buoy robots

## 1 Introduction

There have been many major sea oil spills in recent years. These spills damage not only the ocean environment but also regional economies. Once spilled oil washes ashore, it is difficult to effectively recover it. This results in a high residual amount of spilled oil and long-term damage to the environment as well as to marine and human life. Explosion of offshore oil rig at Gulf of Mexico in 2010 has roused our attention to danger of a large amount of oil spill from subsea oil production systems. On the other hand, once gas blows out from seabed by an accident of subsea oil production system or by a seismic activity and subsea landslide in the area of ample re-serves of methane hydrate in the sea, it seriously damages not only ships and airplanes, but also natural environment.

To prevent oil spills from spreading and causing further damage over wider areas and over time, the spilled oil must be recovered while it is still drifting on the sea surface. An oil

drifting simulation must be carried out to determine where the spilled oil will wash ashore and to adequately deploy oil recovery machines before this occurs. We need the information on the exact location of the drifting oil and the meteorological and oceanographic data around it transmitted in real time so that oil recovery operations can be smoothly coordinated and adequate measures can be taken at coastal areas using information obtained from the oil drifting simulation enhanced by data assimilation.

This paper describes this project from the following viewpoint of the developments of two kinds of robots.

(1) Underwater buoy robot (spilled oil and gas tracking autonomous buoy named SOTAB-I) equipped with a buoyancy control device and two pairs of rotational fins

(2) Multiple floating buoy robots (spilled oil tracking autonomous buoy named SOTAB-II) equipped with sails and sensors to detect oil slicks on the sea surface

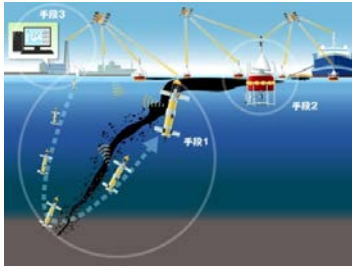


**Fig.1** Autonomous tracking and monitoring system of spilled plumes of oil and gas from seabed

## 2 SOTAB- I

SOTAB-I can move not only in the vertical direction from sea surface to water depth of 2,000m by a buoyancy control device, but also in the horizontal direction by two pairs of rotational fins. It will be tested finally in the areas of Gulf of Mexico and off Niigata where methane gas is spilled. SOTAB-I will be equipped with an underwater mass spectrometer for detecting dissolved gas and oil, other marine environmental sensors, an acoustic velocimeter with altitude sensor, and an acoustic navigation system with an acoustic modem(see Fig. 2). SOTAB-I can move in a wide range both in vertical and horizontal directions.

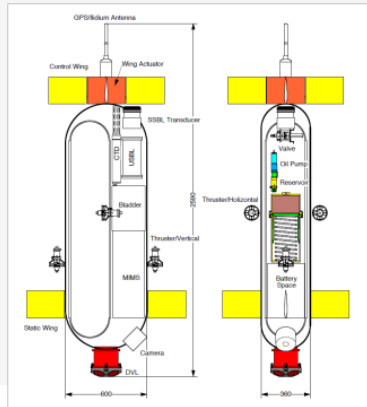


**Fig.2** Illustration of SOTAB-I

### 2.1 Purpose

Spilled Oil and Gas Tracking Autonomous Buoy (SOTAB-I) has the functions of autonomous tracking and monitoring of spilled plumes of oil and gas from seabed. It is equipped with a buoyancy control device, two pairs of rotational fins for guidance and control and sensors to detect dissolved gas and oil.

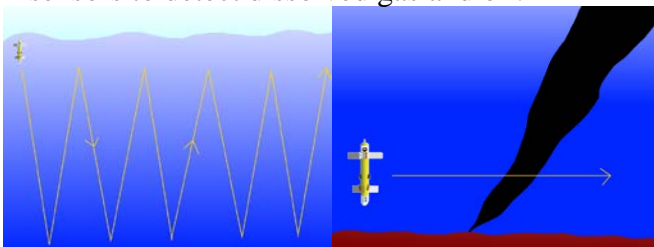


**Fig. 3** Vertical mode

**Fig. 4** Horizontal mode

The guidance simulation was performed for design development of SOTAB-I in this study. SOTAB-I is assumed to have two operation modes. One mode is vertical mode (Fig. 3) which collects the data of the property of the nearby tide and outflow oil while repeating to go underwater and surface. (Fig. 4) Another one is horizontal mode which records the aspect of the outflow oil spot by the equipped photography machine while moving horizontally for a bottom of the sea side in deep sea-bed.

To realize these two operation modes, simulation program was constructed, a vertical experiment carried out and the body fluid differential coefficient using CFD calculation.

### 2.2 Survey modes

SOTAB-I adopts two kinds of motion; vertical mode and horizontal mode. The vertical mode is furthermore composed of two cases. Case I is operated to confirm the properties of the water currents and blew out oil and gas while going along the columnar route (Fig. 5). Case II is operated to survey the detailed characteristics of the plumes by repeating descending and ascending within the plumes. In Figs. 5 and 6, gray area shows plumes of blew out oil and gas, and a yellow line is a trace of SOTAB-I. In addition, Fig. 6 shows that SOTAB-I moves inside vertical section of plumes of oil and gas.

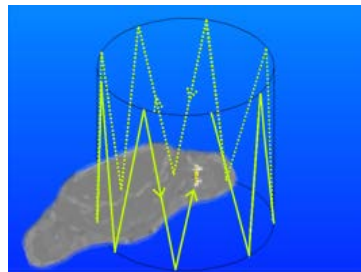


**Fig. 5** Case I



**Fig. 6** Case II

### 2.3 Motion equation and simulation program of the body

To describe a motion equation of the body, I defined the body fixed coordinate system as (Fig. 7). To design a body shape of SOTAB-I, I motion equation about basic simulation model was solved using the Newmark- $\beta$  method. The following two criteria were set up to determine the shape of the body.

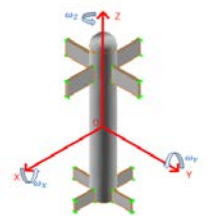


**Fig. 7** Body fixed coordinate system

i) Time necessary for movement between

background up to 2,000m depth and free surface, ii) Horizontal movement distance.

In the case of ii), SOTAB-I gets horizontal driving force by controlling the angles of the movable wings and getting lift. To improve the horizontal maneuverability and to shorten the elapse, a hemispherical shape of the bottom was designed. As a result, drag coefficient decreased, and falling speed became larger.

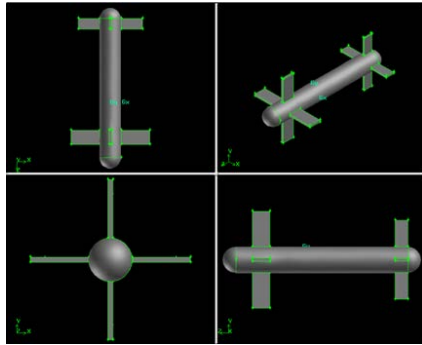


Fig.8 simulation model

Guidance and control was simulated using the model shown in Fig.8.

## 2.4 Vertical mode

### 2.4.1 Vertical mode - case I

Here, it is assumed that an oil and gas blow out accident in the Gulf of Mexico in 2010 is a specific example and oil and gas is distributed in the range from the water depth of 1,500m to the water depth of 500m. Survey along the columnar route was set up.

### 2.4.2 Simulation results on elapse time for survey

It took approximately 19 hours to survey along the columnar route with the diameter of 5 km. The total time was approximately 20 hours including the elapse time for descending at the first step and ascending to free surface at the final step. Furthermore, the case of the survey along the columnar route with the radius of 10 km was investigated. In this case, the columnar route was approximated by regular 48 polygons. It took approximately 61.5 hours to return to mother ship.

### 2.4.3 Vertical mode - case II

In this case, survey will be performed so as to trace a specific substance inside the plumes detected during the vertical mode – case I by using an underwater mass spectrometry that

enables in-situ analysis of water within the range of mass ratio up to 200. Unlike case I, SOTAB-I remains in an oil and gas plume for a long time. On the other hand, the spilled oil and gas diffuse horizontally. Because the controlled horizontal movements distance during one ascent and descent decreases, the number of times of the buoyancy adjustment increases. Because the consumption of electricity of the buoyancy control device occupies most of the consumption electricity of the total system, its balance with the battery power should be considered..

## 2.4.4 Simulation result

Two suitable functions were prepared in this simulation to describe the distribution of a plume with the thickness of 100 m and paths of SOTAB-I was investigated assuming that oil and gas are kept in this range. Ascending and descending are switched near the upper and lower boundaries of the plumes. Figure.9 shows the simulation result.

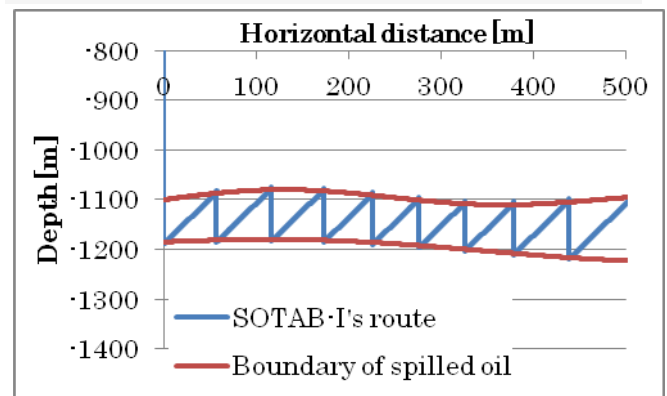


Fig.9 SOTAB-I's route & boundary lines of spilled oil

It would happen that SOTAB-I completely deviates from the existence range of the oil and gas. To prevent such a situation, the survey route can be changed from mother ship using acoustic modem according to rough distribution of the oil and gas obtained in vertical mode –case I.

## 2.5 Horizontal mode

### 2.5.1 Outline of horizontal mode

SOTAB-I is intended to record the state of the blowout scene of the accident in horizontal mode by a camera attached to the bottom of the body. SOTAB-I takes pictures it at distance of about 10m above the blowout spot while moving horizontally along bottom of the sea. It takes pictures multiple times from various directions to confirm the state of the blowout spot. It uses horizontal thrusters and vertical thrusters attached near a center of gravity of body for

horizontal movement and vertical movement, respectively.

### 2.5.2 Estimation of hydrodynamic drag

In this mode SOTAB-I moves horizontally with setting up the body perpendicularly. To estimate the hydrodynamic drag in this situation, CFD analysis was carried out using the following two models. (Figs.10 and 11)

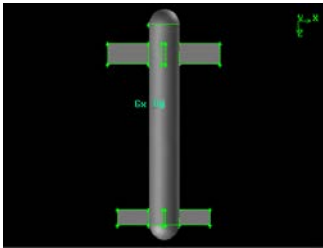


Fig.10 CFD model 1

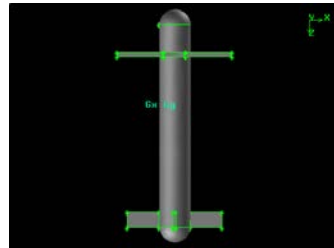


Fig.11 CFD model 2

Figure 10 shows the situation where movable wings keep the initial state (zero degree of wing angle). Figure 11 shows the situation where movable wings keep 90 degrees of wing angle to reduce the hydrodynamic drag on the movable wings. It was confirmed that model 1 has smaller pitching moment than model 2, but has a larger hydrodynamic drag than case 1.

### 2.5.3 Control of the pitching

Both models show negative values of the pitching moment. In other words, it is not possible to control the pitching only by changing the wing angles of the movable wings. Therefore, the position of the thrusters was changed as a method to minimize the pitching. As a result, it was revealed that a pitching moment can be minimized by attaching a thruster to the position 0.288[m] below from the center of gravity. (Fig.12) The model is as below.

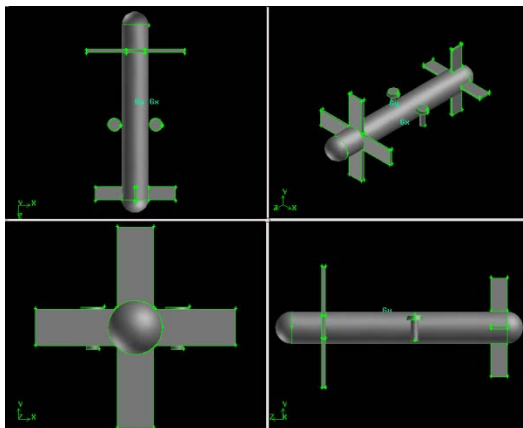


Fig.12 SOTAB-I with thruster

## 3 SOTAB- II

Research and development of Spilled Oil Tracking Autonomous Buoy System (SOTAB-II) has been carried out since 2005(H. Senga, N. Kato, M.Yoshie et al 2009 and 2011). Drifting spilled oil on sea surface has a physical characteristic that it drifts by the effect of wind and water current around it. The recently developed SOTAB- II consists of a cylindrical floating body and an adjustable sail in its area and direction. It was concluded from the results of experiments that the control system of the sail works well, but the present SOTAB-II can't reach the speed of drifting oil. This study designs a new model of SOTAB-II with a yacht shape to reduce the water resistance on it and improve the drifting speed. In the process of the design based on an actual yacht shape, dynamic stability, course stability, scales of break board and sail, maneuverability, and performance of tracking spilled oil on sea surface are considered with supports of CFD analysis and other programs.

### 3.1 Selection of ship type and scale

#### 3.1.1 Battery capacity

First, power consumption of SOTAB-II is calculated as shown in Table 1 to select battery capacity on the assumption that the same sensors, PC control system and sail control system as the present SOTAB-II are used.

Table 1 Power consumption

Devices	Consuming energy[W]
Control board	15
Sail	1
GPS, Current meter, Anemometer etc.	6
Sum	22

Next, battery capacity with a combination of solar cells is determined so that SOTAB-II can operate over one week.

In calculating amount of power solar cells generate, the conditions such as efficiency of power generation and losses of solar cells and batteries should be considered. The conditions shown in Table 2 are used in this simulation. Amount of flux of insolation is taken as that of mean value of all sunny days in April in Osaka.

Table 2 Parameters

Power generating efficiency	13%
Panel loss	87%
Battery loss	80%

As a result, SOTAB-II can be operated one week as shown in Fig.13 by installing 4 Li-ion batteries and solar cells with the area of  $0.6\text{m}^2$ . However, solar cells are considered as supplemental devices for power generation because of those characteristics that those are affected by weather condition easily.

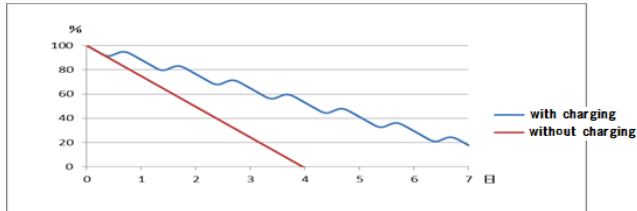


**Fig.13** Decrease of power of battery with and without daily charging of solar cells

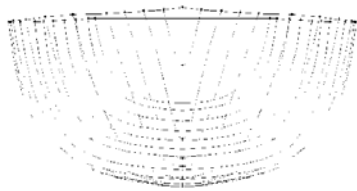


**Fig.14** Body plan of KIT34

**Table 3** Dimensions of KIT34

DIMENSIONS		
HULL		
LOA	m	10.68
LWL	m	8.55
BMAX	m	3.04
BWL	m	2.42
Draft(Canoe body)	m	0.41
Draft(Fin keel)	m	1.94
Displacement(DWL)	kg	3460
Wetted Surface Area	$\text{m}^2$	16.6
GM	m	1.307
Ballast/Displacement Ratio		0.488

And as for rudder, we use the original model as below.



**Fig.15** Rudder

**Table.4** Dimensions of rudder

Chord of blade (Max)	106mm
Length of blade (Max)	280mm
Position of rudder (Position of axis from Midship)	880mm

### 3.1.2 Design of ship form

Large displacement with small ship length is needed to install batteries and sensors. Ship form of sailing yacht "KIT34" designed by Kanazawa Institute of Technology that has broader beam and larger displacement among other sailing yachts with the same ship length. Fig.14 shows the body plan of KIT34. Proper scale of this ship was determined based on the offset data of KIT34.

### 3.1.3 Scale

Because the scale ratio of the designed ship to that of KIT34 becomes large so as to satisfy the required displacement if the original designed waterline is used, waterline around 2m-WL is set up taking the relation between displacement and stability into account.

Table 4 shows dimensions of ships with the scale ratios of 1/10, 1/5, 3/10, and 2/5 comparing with the original dimensions.

**Table 5** Dimensions for Each Scale

DIMENSIONS		original	Scale ratio			
(1) HULL			1/10	2/5	1/5	3/10
LOA	m	10.68	1.068	4.272	2.136	3.204
LWL	m	8.55	1.5	1.6	1.71	2
Displacement(DWL)	kg	3460	3.46	221.44	27.68	93.42
Displacement(2WL)	kg	6570	6.57	420.48	52.56	177.39
Deck Area	$\text{m}^2$	22.48	0.2248	3.598	0.8995	2.024

In addition to mass of devices, mass of ship itself and keel for stability should be considered. It should be noticed that keel was designed iteratively between dynamic stability the principal particulars of the ship including mass of keel. Finally, the scale ratio was determined as 1/5 of the original dimensions.

### 3.2 Stability

By installing the devices, gravity center of SOTAB-II goes up and GM goes down. Because of that, GZ decreases and after all stability gets worse.

Figures 3 and 4 show GZ curve at the unloaded condition and that at the loaded condition,

respectively. These figures show that the angle where GZ becomes zero, namely, the stability vanishes is decreased from 120 deg to 100 deg. Recovering this angle up to 120 deg by installing keel was targeted as the design goal.

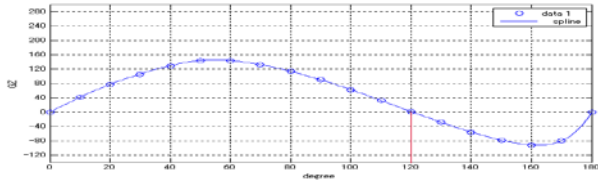


Fig.16 GZ curve at the unloaded condition

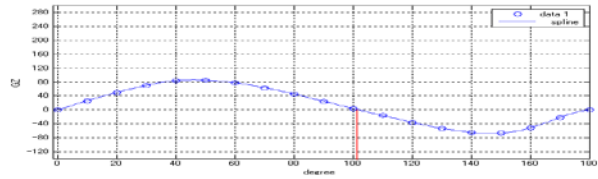


Fig.17 GZ curve at the loaded condition

4 patterns of keel in the form of cylindrical bar made of stainless steel were tested as shown in Table 6. The length of cylindrical bar was set as 510mm. The radius of the cylindrical bar was changed from 15 mm to 25 mm. The distance from the bottom of the ship to gravity center of keel was changed from 220 mm to 320 mm.

Table 6 Results of Simulations

	Radius[mm]	Distance from ship bottom[mm]	Waterline [mm] (2WL=40mm)
(a)	15	320	40.84
(b)	20	220	44.36
(c)	20	320	44.36
(d)	25	320	48.8
	Keel mass[kg]	Gravity center[mm]	Vanishing point of stability
(e)	3.7	37.8	117°
(f)	6.6	27.1	120°
(g)	6.6	15.4	126°
(h)	10.3	-10.3	135°

The results show that installing keel(d) can get the biggest vanishing point of stability. But its weight is more than 10kg, and waterline is over 2WL. Therefore, keel(c) was selected as the most adequate keel, because it can keep an adequate stability and a waterline around 2WL. By installing this keel(c) the vanishing point of stability was recovered to 126 degrees.

### 3.3 Selection of sail and break board

#### 3.3.1 Necessity of brake board

SOTAB-II uses wind power to track floating oil on sea surface. Therefore SOTAB-II needs to

keep the same speed as floating oil. It is known that oil drifts at about 3% of wind speed 10m above sea level.

The recently developed spilled oil tracking autonomous buoy named SOTAB-II consists of a cylindrical floating body and an adjustable sail in its area and direction. It was concluded from the results of experiments that the control system of the sail works well, but the present SOTAB-II can't reach the speed of drifting oil because of large hydrodynamic drag on the cylindrical floating body. This study designs a new model of SOTAB-II with a yacht shape to reduce the hydrodynamic drag on the floating body and improve the drifting speed. So as to keep the new model of SOTAB-II at the same speed of drifting oil, installation of a break board should be considered to control the optimum speed of SOTAB-II.

#### 3.3.2 Wind speed at the sea surface

Wind speed at the sea surface was calculated to analyze the motion of SOTAB-II using the following equations:

$$U(z) = \frac{u^*}{\kappa} \log \frac{z}{z_0} \quad (1)$$

$$u^* = \sqrt{\frac{\tau_s}{\rho_a}} \quad (2)$$

$$\tau_s = \rho_a C_f U_{10}^2 \quad (3)$$

$$C_f = \begin{cases} 1.4 \times 10^{-3} & (0 \leq |U_{10}| < 10) \\ (0.49 + 0.065|U_{10}|) \times 10^{-3} & (10 \leq |U_{10}| < 26) \\ 2.18 \times 10^{-3} & (26 \leq |U_{10}|) \end{cases} \quad (4)$$

Here,  $U(z)$  is the wind speed at the height from sea surface  $z$ ,  $u^*$  is friction velocity at sea surface,  $z_0$  is roughness parameter,  $\kappa$  is Karman constant,  $\tau_s$  is stress of wind,  $\rho_a$  is air density, and  $U_{10}$  is wind speed 10m above sea level.

#### 3.3.3 Analysis of hydrodynamic forces

A CFD software "Fluent" was used to compute hydrodynamic forces.

Assuming that SOTAB-II and oil are on same current, then current effects can be ignored. It is assumed that SOTAB-II drifts at 3% speed of  $U_{10}$ . When SOTAB-II drifts at the speed  $u=0.03U_{10}$ , stream of air and water flows in the posterior direction at the speed  $u$  in the body-fixed coordinate. And stream of wind flows in the anterior direction at the speed of  $U_{0.4} - u$  in the body-fixed coordinate. Here,  $U_{0.4}$  denotes wind speed 0.4m above sea level at which incoming flow speed on the sail is considered (see Fig.18).

To compute hydrodynamic forces exerted by these streams, 3D model of the new body of SOTAB-II was constructed from the offset data of the new body using 3D modeling soft "Gambit," and two types of double hull models were made as shown in Figs.19 and 20 by cutting the 3D model at the waterline. One type shown in Fig.19 was used to compute the hydrodynamic forces acting on the body part below the waterline. The other type shown in Fig.20 was used to compute the hydrodynamic forces acting on the body part above the waterline. Wave drag was treated as negligible because SOTAB-II drifts slowly.

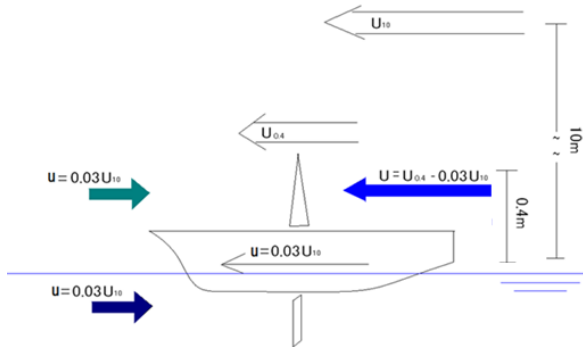


Fig.18 Relations of streams

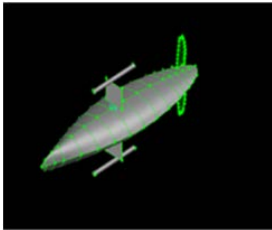


Fig.19 Double hull of lower side

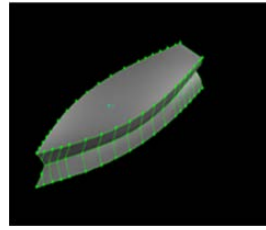


Fig.20 Double hull of upper side

### 3.3.4 Design of brake board

SOTAB-II should keep its speed at 3% of wind in any situations. Therefore, the scale of brake board was designed so that the hydrodynamic force acting on the sail and that acting on the upper side of body in the stream of air in the posterior direction are balanced under the severest condition of the wind speed of 50m/s corresponding to a very strong typhoon.

On the other hand, brake board is not necessary when SOTAB-II is guided by a thruster, because the brake board acts as a load. Therefore, two ways of the usage of brake board are taken; one way in expanding the brake board during the operation of SOTAB-II autonomously tracking spilled oil, the other way by folding the brake board during the operation of SOTAB-II guided to a far target point using a thruster.

### 3.3.5 Design of sail

Sail has to generate thrust force to make SOTAB-II drift at the speed of 3% of wind in any situations. Then, method of design of sail is different from break board. Normal condition where wind speed is 3m/s was set up under the assumptions that sail is adjustable and 50% of sail area is set as basis in its design. Table 7 shows wind speed and the related speeds. Table 8 shows 3 patterns of dimensions of sail with a triangular shape.

Table 7 Values used in calculation

$U_{1.0}$	3.0 m/s
$U_{0.4}$	1.42 m/s
$u$	0.09 m/s
$U$	1.33 m/s

Table 8 3 patterns of dimensions of sail

	height[mm]	base[mm]
(A)	212	212
(B)	250	250
(C)	300	300

Table 9 Hydrodynamic forces against types of sails

Hydrodynamic forces [N]	(A)	(B)	(C)
Upper part	0.0777	0.0909	0.112
Lower part	-0.115	-0.115	-0.115
Sum	-0.0375	-0.0243	-0.003

Table 13 shows the hydrodynamic forces acting on upper part and lower part for three types of sails. We can see that the hydrodynamic forces acting on upper part and lower part are balanced for sail(C).

Sail(C) was evaluated from the viewpoint if SOTAB-II equipped with it can be operated in any situations. To do it, wind thrust forces by sail in the furled and full conditions and water

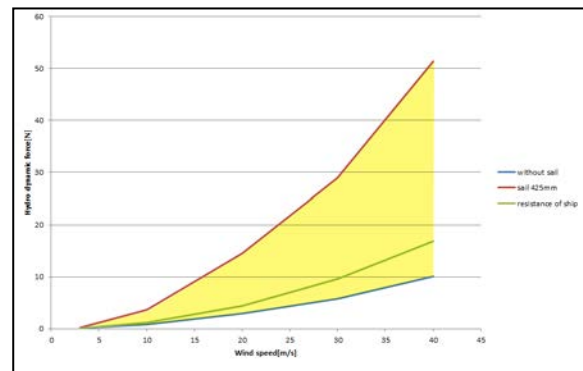


Fig.21 Wind thrust forces by sail in the furled and full conditions and water resistance acting on the lower body

resistance acting on the lower body were computed for the wind speeds of 3m/s, 10m/s, 20m/s, 30m/s and 40m/s as shown in Fig.21.

In Fig.21 red line shows the wind thrust force by full sail, blue line shows the wind thrust force by furled sail, and green line shows water resistance of SOTAB-II. Yellow region in Fig.21 indicates that thrust force can be generated by controlling sail area. As the values of the water resistance is located within the yellow region for the overall region of the target wind speeds, we can judge that sail(C) can fulfill the operational condition of SOTAB-II for the wind speed from 3m/s to 40m/s.

### 3.4 Maneuverability

Because drifting speed of SOTAB-II with about 3% of wind speed is slow, hydrodynamic forces acting on the rudder is small. It leads to weak maneuverability of SOTAB-II. To increase the maneuverability, jib sail that has a self-stabilizing function against the change of wind direction like a weathercock is installed at the front of SOTAB-II.

Performances of rotation of SOTAB-II equipped with jib sail in the form of rectangular triangle (base\*height=40mm\*40mm) were evaluated comparing rotation with and without steering. The motion was simulated after wind direction was changed by 20 degrees as shown in Fig.22.

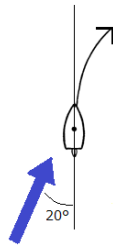


Fig.22 Schematic of evaluation of rotation in wind

Fig.23 shows the comparison of trajectory with and without steering of deg. From Fig.22 we can see that rotation with steering is more effective than that without steering.

Fig.24 shows the configuration of new SOTAB-II based on the above-mentioned discussions.

### 4 Concluding remarks

Sea experiments will be carried out using SOTAB-I in the areas of Gulf of Mexico and off Niigata where methane gas is spilled, and using SOTAB-IIs in the area of Norway where actual oil is dispersed.

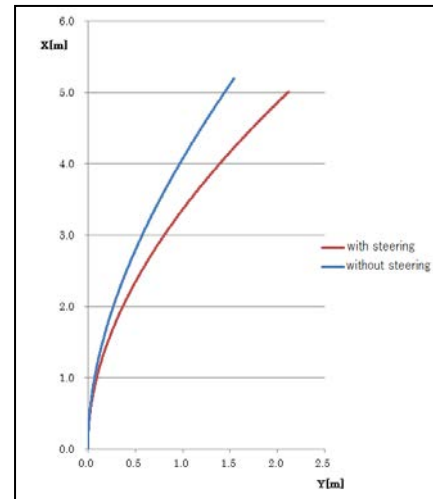


Fig.23 Effect of steering on maneuverability

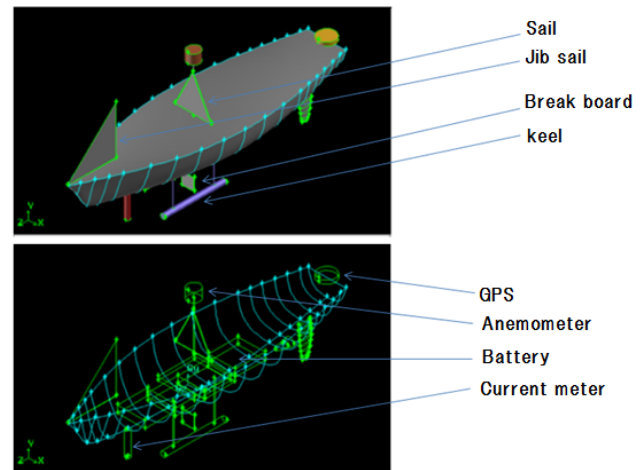


Fig.24 Configuration of new SOTAB-II

### Acknowledgements

This research project is being funded for 2011FY-2015FY by Grant-in-Aid for (Scientific Research(S) of Japan Society for the Promotion of Science(No. 23226017).

### References

- <http://www.naoe.eng.osaka-u.ac.jp/~kato/project/>
- H. Senga, N. Kato, M.Yoshie et al., Spilled Oil Tracking Autonomous Buoy System, J. of Advanced Robotics, Vol.23, pp.1103-1129, 2009
- H. Senga, N. Kato, H. Suzuki, M. Yoshie, T. Tanaka et al., Development of a New Spilled Oil Tracking Autonomous Buoy, Marine Technology Society Journal, Vol.45, No.2, pp.43-51, 2011